Journal of King Saud University - Science 36 (2024) 103488

HOSTED BY

Contents lists available at ScienceDirect

Journal of King Saud University - Science

journal homepage: www.sciencedirect.com

Full Length Article

Effects of *Laurus* extract against cadmium-induced neurotoxicity in rats

Hanaa M. Hassan [a], Hanaa S.S. Gazwi [a,*], Inas Hussein Refaat [b], Asmaa Hussein Zaki [a], Marija Milošević [c], Salim S. Al-Rejaie [d], Mohamed Mohany [d], Eman E. Yassien [a]

[a] Department of Agricultural Chemistry, Agriculture Faculty, Minia University, El-Minia, Egypt
[b] Department of Zoology and Entomology, Faculty of Science, Minia University, Minia 61519, Egypt
[c] Institute for Information Technologies, University of Kragujevac, Kragujevac 34000, Serbia
[d] Department of Pharmacology and Toxicology, College of Pharmacy, King Saud University, P.O. Box 55760, Riyadh 11451, Saudi Arabia

ARTICLE INFO

Keywords:
Laurus
Cd
FRAP
GC–MS
HLPC
LDH
SOD
AChE

ABSTRACT

Cadmium (Cd) is a hazardous heavy metal with widespread environmental presence, posing significant threats to human and animal health. This study investigates the neurotoxic effects of Cd exposure and explores the therapeutic efficacy of *Laurus nobilis* L. in counteracting these adverse effects. Cd exposure induces oxidative stress and neurotoxicity, leading to neuronal damage and histopathological alterations. *Laurus*, known for its antioxidant properties, is assessed for its potential in mitigating Cd-induced neurotoxicity through in vitro antioxidant assays, GC–MS analysis, HPLC profiling, and experimental animal models. Results demonstrate that *Laurus* ethanolic extract exhibits significant antioxidant activity, attributed to its phenolic and flavonoid constituents. GC–MS analysis reveals various bioactive compounds in the extract, including Hexadecanoic acid methyl ester and (Z)-13-Docosenamide, which posses neuroprotective properties. HPLC analysis identifies phenolic compounds such as ellagic acid and flavonoids like rutin and kaempferol in the extract. In vivo studies in rats exposed to Cd demonstrate that *Laurus* extract administration mitigates Cd-induced alterations in body and brain weight, hematological parameters, liver and kidney function, oxidative stress markers, and acetylcholinesterase (AchE) activity. Histopathological examination confirms the protective effects of *Laurus* against Cd-induced neuronal damage. The SOD model, validated with high resolution (2.05 Å) and strong R values (work: 0.192, free: 0.236, observed: 0.194), shows strong structural stability (C-score: 0.30). Docking studies reveal high binding affinities of kaempferol (−8.1 kcal/mol) and rutin (−8.7 kcal/mol) with SOD with kaempferol demonstrating superior solubility, lipophilicity, and drug-likenessSimulation analysis confirms the protein's flexibility and adaptability, highlighting its therapeutic potential, especially with kaempferol. These findings suggest the therapeutic potential of *Laurus*. as a natural remedy for Cd-induced neurotoxicity, highlighting its antioxidant and neuroprotective properties.

1. Introduction

Cadmium is a heavy metal that the body does not need and is known to be toxic to humans (Genchi et al., 2020). It is currently considered the seventh most hazardous chemical for human health, based on its toxicity and the frequency of human exposure (ATSDR, 2022). In addition to workplace exposure, people can come into contact with cadmium through food, cigarette smoke, and polluted air. Cadmium accumulates in the human body, particularly in the kidneys and liver, and has a half-life of 25–30 years because it is not easily excreted. This metal can enter cells by mimicking zinc, utilizing zinc transporters and calcium channels in a process referred to as the "Trojan horse" mechanism (Thévenod et al., 2019; MGenchi et al., 2020). Once inside, cadmium can replace zinc, iron, and copper in many proteins, causing oxidative stress, DNA damage, endoplasmic reticulum (ER) stress, mitochondrial dysfunction, and autophagy (Ma et al., 2022).

Cadmium has been identified as neurotoxic, as reported by Wang and Matsushita (2021) and Ruczaj and Brzóska (2023). This heavy metal has been found to accumulate in different brain regions, particularly in the locus ceruleus neurons of individuals with various clinicopathological conditions and causes of death (Pamphlett et al., 2018). Environmental exposure to cadmium is suggested to damage the nervous system and contribute to neurodegenerative diseases like Alzheimer's, Parkinson's, and amyotrophic lateral sclerosis (Ruczaj and Brzóska, 2023). Studies

* Corresponding author.
E-mail address: hanaa.saleh@mu.edu.eg (H.S.S. Gazwi).

https://doi.org/10.1016/j.jksus.2024.103488
Received 9 August 2024; Received in revised form 4 September 2024; Accepted 14 October 2024
Available online 18 October 2024

have also shown that cadmium can induce apoptosis in motor neurons from human embryonic spinal cord explants (Sarchielli et al., 2012) and in the olfactory bulbs of animals exposed through diet or inhalation (Sunderman, 2001). Also, Recent studies reveal that cadmium exposure can impair cognitive function (Sasaki and Carpenter, 2022; Deng et al., 2023).

Medicinal plants and commercially produced natural products have a significant and extensive impact in mitigating the adverse consequences resulting from exposure to environmental contaminants, medicinal plants like *Laurus* have gained attention for their therapeutic potential (Almeer et al., 2019). Known for its antioxidant properties (Vardapetyan et al., 2013), *Laurus* has been extensively studied for its ability to alleviate oxidative disorders related to stress, attributed to its rich phenolic and flavonoid content (Hassan et al., 2019). *Laurus* nobilis L., commonly referred to as laurel, is not only a popular culinary herb for its flavor and aroma but is also recognized for its medicinal benefits, including its effectiveness in treating diseases, nerve pain, and intestinal spasms (Chaudhry and Tariq, 2006). Laurel leaf extract has also shown potential in preventing neurotoxicity induced by lead exposure (Gazwi et al., 2020).

This study aimed to explore the therapeutic efficacy of *Laurus* in counteracting adverse brain effects induced by Cd.

2. Materials and methods

2.1. Extract Preparation

The ethanol extract of *Laurus* leaves was prepared following the method of Malti and Amarouch (2009).

2.2. In vitro antioxidant Activity

The antioxidant action of the *Laurus* ethanolic extract was assessed using FRAP and ABTS assay of the ethanolic extract of *Laurus* were determined according to the method of Benzi et al. (1996) and Arnao et al. (2001), respectively.

2.3. GC–MS Analysis

GC/MS analysis of the extract was performed using a Thermo Scientific TG-5MS fused silica capillary column at the National Research Center's mass spectrometry (Dokki, Giza). Analysis conditions included an electron ionization system with 70 eV ionization energy, helium carrier gas at 1 mL/min flow rate, and injector and MS transfer line temperatures at 280° C. Quantification of identified components utilized percent relative peak area. Tentative identification of compounds relied on comparing their relative retention times and mass spectra with those in the NIST and WILLY library data of the GC/MS (Adams, 2007).

2.4. HPLC analysis

The phenolic and flavonoid components of *Laurus* extract were determined using a HPLC system (Agilent 1100; Santa Clara, CA, USA). All samples, standard solutions, and the mobile phase were degassed and filtered through a 0.45 μm membrane filter (Millipore). Compound identification was achieved by comparing their retention times and UV absorption spectra with those of known standards and a UV/Vis detector at a wavelength of 230–400 nm were used to determine the extract's phenolic and flavonoid components. The extract was injected set at 20 μL, and a reversed-phase C18 column measuring 2.5 × 30 cm was used. The mobile phase consisted of 0.05 % trifluoroacetic acid in acetonitrile with water. The mixing ratios for solvents A and B at different time points were as follows: at 0.000 min, 18.0 % A and 82.0 % B; at 5.000 min, 20.0 % A and 80.0 % B; at 12.000 min, 40.0 % A and 60.0 % B; and at 20.000 min, 18.0 % A and 82.0 % B. The flow rate was maintained at 1.0 ml/min, and the temperature was kept at 25 °C. Detection was performed using a diode array detector (Biswas, 2013).

2.5. Experimental Design

Thirty-two male albino Sprague-Dawley rats, aged 2 months and weighing 180 ± 8 g, were acclimatized for two weeks in the Chemistry Department's Biological Laboratory at the Faculty of Agriculture, Minia University, Egypt. They were housed in standard conditions with a regular diet and were randomly divided into four groups (8 rats per group) after acclimatization:

Group 1 (Control): Healthy rats.

Group 2 (*Laurus*): Rats received *Laurus* at 250 mg/kg b.wt/day (Ravindran et al., 2013).

Group 3 (Cd): Rats received Cd at 5 mg/kg b.wt/day (Renugadevi and Prabu, 2010).

Group 4 (*Laurus* + Cd): Rats were pre-treated with *Laurus* (250 mg/kg b.wt/day) 30 min before Cd administration at a dose of 5 mg/kg b.wt / day.

For a 30-day period, each group of rats received daily oral administration of their respective treatments. Post-treatment, blood samples were collected and divided into two parts. The first part was used for hematological and biochemical analyses, while the second underwent centrifugation at 3000 rpm for 15 min. The serum obtained was then stored at −20 °C for future biochemical analysis.

All tests were carried out in accordance with the guidelines provided by the ethics committee for the Faculty of Agriculture, Agriculture Chemistry department, Minia, Egypt, in accordance with the Ethics Committee's guidelines for using animals in research (Approval No. **MU 015/04/23**). The study was conducted in accordance with the local legislation and institutional requirements.

2.5.1. Hematological Parameters

Red blood cells (RBCs), white blood cells (WBCs), and hematocrit values (HCT %) or packed cell volume (PCV) were analyzed as per the protocol of Dacie and Lewis (1991). Hemoglobin concentration (Hb) was measured according to the method described by VanKampen and Zijlstra (1961). The percentage of each leukocyte type in relation to the total WBC count was determined following Schalm et al. (1975).

2.5.2. Biochemical methods Analysis

Aspartate aminotransferase (AST) and alanine aminotransferase (ALT) were measured in serum using the colorimetric method of Reitman and Frankel (1957). Urea and creatinine levels were assessed in serum according to the methods of Fawcett and Scott (1960) and Murray (1984), respectively. Alkaline phosphatase (ALP) activity was measured in serum colorimetrically according to Belfield and Goldberg (1971). Total and direct bilirubin levels were determined in serum colorimetrically following the method of Walters and Gerarde (1970).

2.5.3. Tissue Samples

Post-euthanasia, organs including the brain were collected for analysis. A portion of the brain tissue was fixed in 10 % formalin solution and stored in 70 % ethanol for histopathological examination. Other brain tissue samples were homogenized for analysis and measurement of malondialdehyde (MDA) levels and antioxidant enzymes (superoxide dismutase (SOD) and catalase (CAT)), following the methods of Draper and Hadley (1989), Nishikimi et al. (1972), and Aebi (1984), respectively. Acetylcholinesterase (AChE) activity was quantified using cholinesterases kits, as per Ellman et al. (1961).

2.5.4. Histopathological Determinations

Samples of brain tissue from both control and treated groups were fixed in neutral buffered 10 % formalin. Post-fixation, they were washed, dehydrated through graded alcohol series, and embedded in paraffin. Sections of 4–5 μm thickness were cut from these samples and stained with hematoxylin and eosin. The stained sections were then

examined under a microscope for histopathological changes (Banchroft et al. 1996).

2.6. Insilco analysis

In this research, a combination of approaches was implemented to evaluate drug-like properties, study protein–ligand interactions, as well as to investigate binding affinity and mode of action of ligands to proteins. To delve into the conformational changes of the molecules and to observe the dynamic behavior of the protein–ligand complexes over time, we employed MD simulations as per the method of earlier researchers (Huey et al., 2018). Multiple docking simulations were studied using AutoDock (Morris et al., 2009), to model protein–ligand complexes, predict putative binding sites, and analyze binding pose and binding affinity. Docking simulations and binding site predictions were carried out to better characterize the interactions between molecules using the iMode web server web server (Lauria et al., 2019). We use PyMOL and Chimaera as per the method by Le et al. (2019) for examining the conformation variations during the binding of ligands and proteins. The aim was to forecast changes that result from the process of chaining. We also carried out further analyses of the binding mode and the predicted involved binding sites using the PyLip web server (Pires et al., 2019) as described in Pires et al., 2019. Based on the ADMET screening, Ligands could be predicted as a druglike molecule, which is future described that it can exhibit desired action that interacts in vivo under physiological conditions to which the compound is administered. This analysis verified the pharmacological similarity of the compounds (Cheng et al., 2020).

2.7. Statistical Analysis

The experimental results were presented as mean ± standard deviation (SD) for three parallel measurements. Analysis of variance (ANOVA) procedures were applied for statistical analysis. GraphPad Prism®, a product of GraphPad Software, San Diego, CA, USA, was utilized for statistical calculations (Motulsky, 1999).

3. Results

3.1. In vitro antioxidant activity of ethanolic extract of Laurus

The ethanolic extract of *Laurus* demonstrated substantial antioxidant activity through radical scavenging assays like ABTS and FRAP, essential for evaluating antioxidant capacity.

The ABTS assay, reflecting antioxidant capacity (Wu et al., 2006), showed that the *Laurus* extract had notable ABTS radical scavenging activity, with a value of 751.63 µM TE/mg extract (Table 1). The FRAP value of the *Laurus* extract was 252.64 µM TE/mg, indicating its electron donation capacity to stabilize free radicals in food and biological systems (Table 1).

3.2. GC–MS analysis

The GC–MS analysis of the *Laurus* ethanol extract revealed various compounds, as detailed in Table 2 and Fig. 1. Notable among these compounds is Hexadecanoic acid, methyl ester (methyl palmitate), an organic compound. Additionally, (Z)-13-Docosenamide was found which a long-chain fatty acid amide found in plants, insects, and mammals, Also other significant compounds found in the *Laurus* extract include Santamarine and Reynosin, sesquiterpene lactones.

Table 1
Antioxidant activity using FRAP and ABTS assay of *Laurus* ethanol extract.

Tests	*Laurus* ethanol extract
FRAP (µM TE / mg Extract)	252.64 ± 5.31
ABTS (µM TE / mg Extract)	751.63 ± 44.1

Data represent the mean ± S.D. of observations from six replicates.
TE Trolox equivalent.

Table 2
The major phytocomponents present of ethanolic leaves extract of *Laurus* using GC–MS analysis.

NO	RT	Compound Name	MF	MW	Area %
1	48.30	Hexadecanoic acid, methyl ester	$C_{17}H_{34}O_2$	270	11.8
2	48.89	Azuleno(4,5-b)furan-2(3H)-one decahydro-3,6,9-tris (methylene)-, (3aS-(3aà,6aà,9aà,9bá))-	$C_{15}H_{18}O_2$	230	3.68
3	54.31	Santamarine	$C_{15}H_{20}O_3$	248	2.83
4	54.68	Octadecanoic acid, methyl ester	$C_{19}H_{38}O_2$	298	9.93
5	55.21	Reynosin	$C_{15}H_{20}O_3$	248	4.12
6	58.84	2-(3-Hydroxy-2-nitro-1-phenyl butyl)cyclohexanone	$C_{14}H_{17}NO_3$	247	1.27
7	73.37	13-Docosenamide, (Z)-	$C_{22}H_{43}NO$	337	10.71
8	74.64	Tris(2,4-di-*tert*-butylphenyl) Phosphate	$C_{42}H_{63}O_4P$	663	1.19
9	75.45	silane, trimethyl(((3á)-stigma st-5-en-3-yl)oxy)-	$C_{32}H_{58}OSi$	487	1.10
10	77.63	9,12-octadecadienoic acid (z,z)-,2,3-bis((trimethylsilyl) oxy) propyl ester	$C_{27}H_{54}O_4Si_2$	499	1.01
11	81.45	Vitamin E	$C_{29}H_{50}O_2$	431	1.42

RT: Retention Time **MF:** Molecular Formula **MW:** Molecule Weight.

3.3. HPLC analysis

The analysis of the sample revealed the presence of various phenolic compounds, emphasizing their potential as bioactive agents with significant pharmaceutical and therapeutic applications. Fig. 2 and Table 3 shows the High-Performance Liquid Chromatography (HPLC) chromatogram, which highlights the detection of several phenolic compounds in the sample. The analysis indicated that phenantherine was the most abundant, with a concentration of 18.2 µg/g. Other identified phenolic compounds include Coumaric (4.4 µg/g), ellagic acid (3.0 µg/g), resorcinol (1.5 µg/g), chlorogenic acid (0.6 µg/g), Cinnamic (0.5 µg/g), vanillic acid (0.3 µg/g), ferulic acid (0.1 µg/g), and Pyrochatechol (0.1 µg/g), as illustrated in Fig. 2 and Table 3.

The flavonoid profile of the sample was comprehensively analyzed, revealing the presence of several key flavonoid compounds. The analysis identified kaempferol as the most abundant flavonoid, with a concentration of 135.84 µg/g. Other detected flavonoids include rutin (58.66 µg/g), quercetin (38.06 µg/g), hesperidin (15.58 µg/g), and apigenin (0.1274 µg/g), as detailed in Table 3 and Fig. 3. These flavonoids are known for their antioxidant properties and contribute significantly to the therapeutic potential of the sample, supporting its use in various health-related applications.

3.4. Body weight gain and brain weight

Table 4 shows significant differences in body weight gain and brain weight among groups. Cd exposure led to a notable reduction in body weight gain and brain weight ($p < 0.05$) compared to the control group. Rats pretreated with a combination of *Laurus* extract and Cd showed a significant improvement in both body weight gain and brain weight compared to the Cd-only group.

3.5. Hematological findings

The hematopoietic system, highly susceptible to toxicity, showed significant alterations in our study (Table 5). In the Cd group, there was a notable decrease in RBC count, Hct, Hb levels, and PLT count compared to the control group ($p < 0.05$).

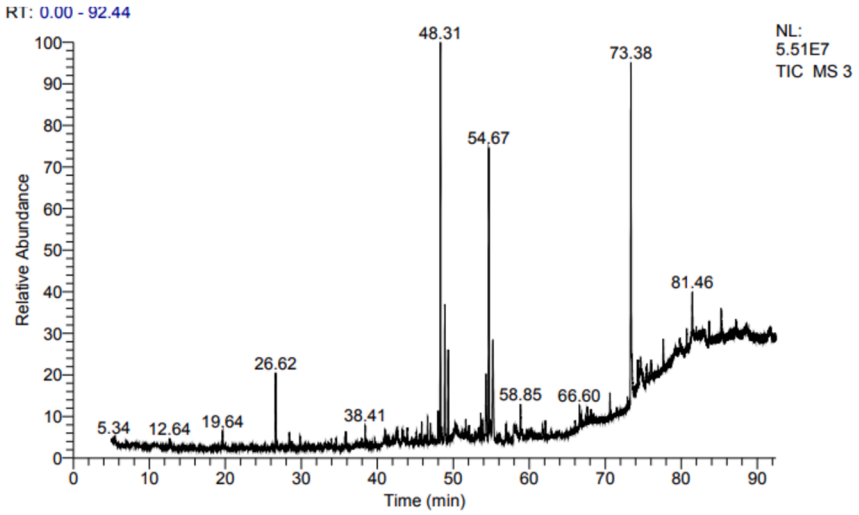

Fig. 1. GC–MS chromatogram of compounds identified in *Laurus* extract.

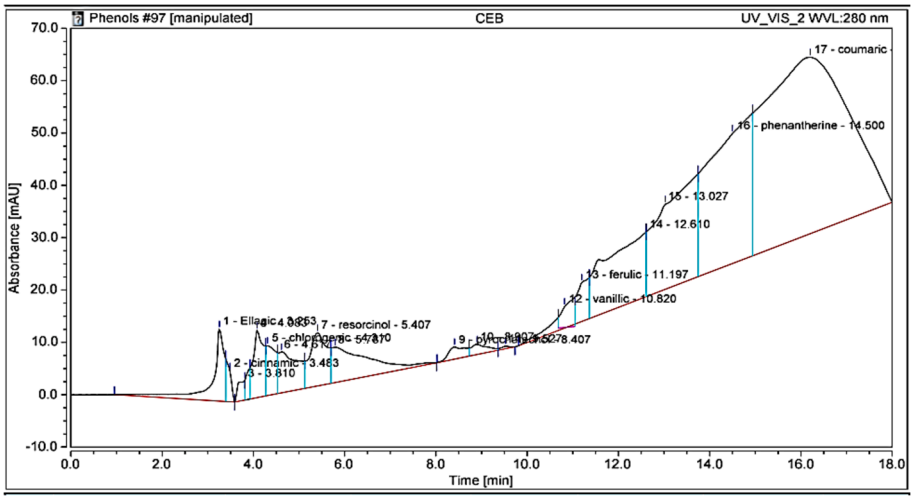

Fig. 2. HPLC chromatogram of phenolic compounds identified in ethanol extract of *Laurus*.

Table 3
Chemical composition analysis of phenolic and flavonoid compounds of ethanol extract from *Laurus* by HPLC.

Components	RT (min)	Conc (µg/g)
Phenolic Compounds		
Ellagic	3.253	3
Cinnamic	3.483	0.5
Chlorogenic	4.310	0.6
Resorcinol	5.407	1.5
Pyrochatechol	8.407	0.1
Vanillic	10.820	0.3
Ferulic	11.197	0.1
Phenantherine	14.500	18.2
Coumaric	16.207	4.4
Flavonoids Compounds		
Apiginin	4.6	0.1274
Rutin	5.2	58.6617
Hesperidin	8.1	15.5859
Kaempferol	9.0	135.8448
Quercetin	10.0	38.0600

Furthermore, the Cd-exposed group exhibited a significant increase in WBCs and neutrophils, while lymphocytes markedly decreased ($p < 0.05$) (Table 5).

On the other hand, *Laurus* treatment ameliorated these hematological alterations, showing protective effects against RBC degradation caused by Cd.

3.6. Biochemical assay

Table 6 presents the effects of *Laurus* extract on blood biomarkers reflecting the health status and organ integrity in cadmium-treated albino rats. Compared to the Control and *Laurus* groups, the Cadmium group showed significant elevations in AST, ALT, ALP, total bilirubin, direct bilirubin, urea, creatinine, and LDH levels, indicating liver and kidney damage.

In contrast, the *Laurus* + Cadmium group, where *Laurus* extract was administered alongside cadmium, showed noticeable reductions or mitigations in these biomarker levels.

3.7. Oxidative stress

Exposure to cadmium (Cd) significantly increased oxidative stress ($p < 0.05$), as shown by elevated lipid peroxidation (MDA) and reduced

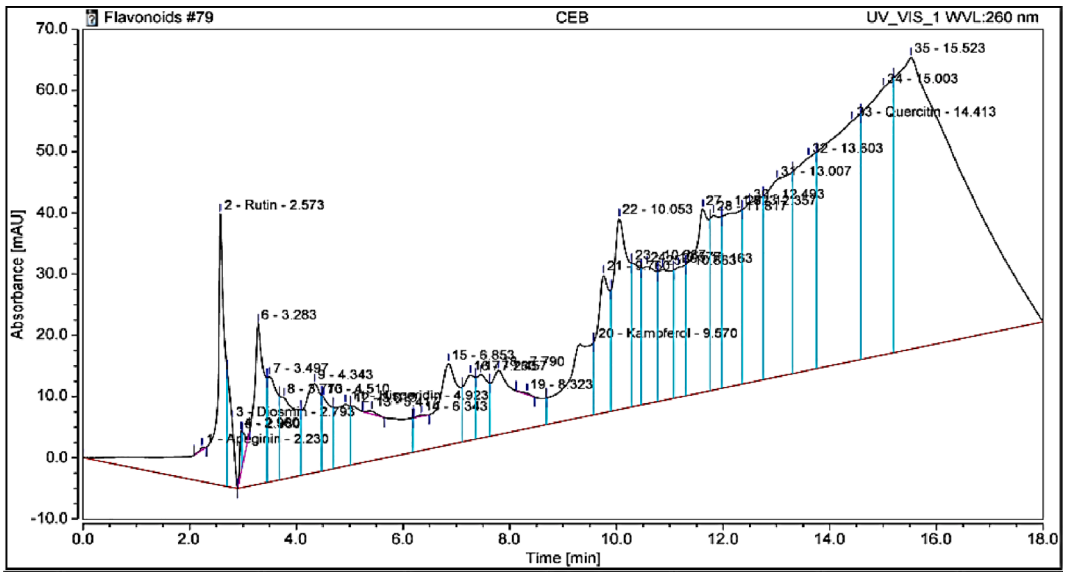

Fig. 3. HPLC chromatogram of flavonoid compounds identified in *Laurus* extract.

Table 4
Effects of *Laurus* Extract on Body Weight Gain and Brain Weight in Cd-Treated Albino Rats.

	Control	*Laurus*	Cd	*Laurus* + Cd
Body weight gain (g)	26.75 ± 0.50	22.25 ± 1.71	15.50 ± 0.57[a]	19.50 ± 0.57[ab]
Brain wt.(g)	1.54 ± 0.02	1.44 ± 0.03	0.98 ± 0.03[a]	1.300 ± 0.01[ab]

Data indicate the mean ± S.D. for observations from 8 rats. [a] Significantly different from control group. [b] Significantly different from Cd group.

Table 5
Effects of *Laurus* extract on some hematological characteristics picture in Cd treated albino rats.

	Control	*Laurus*	Cadmium	*Laurus* + Cadmium
RBC count (106/µL)	4.55 ± 0.21	4.67 ± 0.17	2.93 ± 0.25[a]	3.55 ± 0.13[ab]
WBC count (103/µL)	3.70 ± 0.18	4.350 ± 0.26	10.88 ± 0.34 [a]	5.00 ± 0.22 [ab]
Hemoglobin (g/dL)	13.6 ± 0.22	14.08 ± 0.27	8.90 ± 0.33[a]	12.18 ± 0.59[ab]
Hematocrit (%)	39.45 ± 0.52	40.68 ± 0.57	30.08 ± 0.27[a]	34.53 ± 0.76[ab]
Lymphocyte (10^9/L)	3.78 ± 0.18	3.85 ± 0.24	1.69 ± 0.10[a]	2.44 ± 0.14[ab]
Monocyte (10^9/L)	0.33 ± 0.02	0.29 ± 0.01	0.19 ± 0.01[a]	0.24 ± 0.01[ab]
Neutrophils (10^9/L)	1.06 ± 0.03	1.03 ± 0.52	2.12 ± 0.05[a]	1.25 ± 0.05 [ab]
PLT(10^9/L)	567.5 ± 2.08	464 ± 3.37	329.50 ± 3.41[a]	445 ± 1.71[ab]

Data indicate the mean ± S.D. for observations from 8 rats. [a] Significantly different from control group. [b] Significantly different from Cd group.

levels of catalase (CAT) and superoxide dismutase (SOD). The administration of *Laurus* extract significantly reversed Cd-induced changes (Table 7).

3.8. Acetyl cholinesterase

Rats exposed to cadmium (Cd) displayed a notable decrease in acetylcholinesterase (AChE) activity in their brain tissue compared to the control group, as shown in Table 8. Treatment with *Laurus* extract significantly improved AChE activity ($p < 0.05$) compared to Cd-exposed rats, as shown in Table 8.

Table 6
The effect of *Laurus* extract on some biochemical parameters in Cd treated albino rats.

	Control	*Laurus*	Cadmium	*Laurus* + Cadmium
AST (U/ml)	60.50 ± 5.51	71.00 ± 2.58	206.8 ± 4.031[a]	108.3 ± 7.27[ab]
ALT (U/ml)	32.33 ± 1.51	45.33 ± 2.51	77.33 ± 2.51[a]	52.67 ± 2.52[ab]
ALP (U/ml)	86.75 ± 1.71	84.50 ± 3.11	157 ± 2.16[a]	108.5 ± 1.29[ab]
Total Billirubin (mg/dl)	0.32 ± 0.02	0.3875 ± 0.03	0.98 ± 0.02[a]	0.69 ± 0.02[ab]
Direct Billirubin (mg/dl)	0.13 ± 0.013	0.14 ± 0.005	0.21 ± 0.013[a]	0.16 ± 0.008[ab]
Urea (mg/dl)	4.65 ± 0.21	4.70 ± 0.12	5.800 ± 0.22[a]	4.800 ± 0.22[b]
Creatinine (mg/dl)	0.83 ± 0.05	0.89 ± 0.03	1.39 ± 0.01[a]	1.056 ± 0.03[ab]
LDH (U/l)	865.5 ± 2.65	920.80 ± 0.96	2053 ± 2.58[a]	1985 ± 9.71[ab]

Data indicate the mean ± S.D. for observations from 8 rats. [a] Significantly different from control group. [b] Significantly different from Cd group.

Table 7
Effect of *Laurus* extract on oxidative stress in brain homogenate of cadmium (cd)-treated albino rats.

	Control	*Laurus*	Cadmium	*Laurus* + Cadmium
SOD (U/ml)	285.3 ± 2.22	287.5 ± 3.69	109.3 ± 2.2[a]	212.0 ± 5.16[ab]
CAT (U/g protein)	0.97 ± 0.02	0.98 ± 0.02	0.59 ± 0.03[a]	0.82 ± 0.03[ab]
MDA (nmol/g)	50.41 ± 0.17	52.68 ± 0.94	100.7 ± 1.15[a]	67.38 ± 0.96[b]

Data indicate the mean ± S.D. for observations from 8 rats. [a] Significantly different from control group. [b] Significantly different from Cd group.

Table 8
The Effect of *Laurus* extract on AChE activity in brain homogenate of cadmium (cd)-treated albino rats.

	Control	*Laurus*	Cadmium	*Laurus* + Cadmium
AChE activity (pg/ml)	113.5 ± 2.08	100 ± 0.82	84.25 ± 1.7 [a]	89.00 ± 0.82 [ab]

Data indicate the mean ± S.D. for observations from 8 rats. [a] Significantly different from control group. [b] Significantly different from Cd group.

3.9. Histopathological examination of brain

Microscopically, the control group rats showed a typical histological structure (cerebral cortex). Also, the Laurus group's rat brain did not show any histopathological changes Conversely, tissue sections from the Cd-exposed group exhibited neuronal necrosis (arrow), focal gliosis, and neuronophagia. Pre-treatment with Laurus significantly ameliorated the cortical abnormalities induced by Cd exposure (arrow) (Fig. 4 and Table 9).

3.10. Insilco analysis

3.10.1. SOD model analysis and Validation

SOD shows a strong molecular structure with a resolution of 2.05 Å, SOD was selected for further analysis by X-ray diffraction. The high resolution allows for accurate identification of the molecular structure by allowing an exhaustive and precise analysis of its many complexities. The strong correlation of the improved model (R values) with the experimental data provides additional evidence of the accuracy of the structure. The results demonstrate a high level of precision and reliability, as shown by the R values for work (0.192), free (0.236), and observed (0.194). Once the molecular composition is identified, it provides a solid foundation for future research. The selected SOD model, which had a C-score of 0.30, was uploaded to the iMod server and displayed in four unique modes, as seen in Fig. 5. The selected model has a high degree of structural stability, as shown favorable C-score and normal Z-score. Secondary structure representation often shows a helical appearance, highlighting possible binding locations and functional regions.

Table 9
The severity of histological changes in brain (cerebral cortex).

Histopathological lesion	Control	*Laurus*	Cadmium	Cadmium + *Laurus*
Necrosis of neurons	–	–	+++	+
Neuronophagia	–	–	++	+
Focal gliosis	–	–	++	–

(–) no change (+) mild change (++) moderate change (+++) severe change.

3.10.2. Docking study

Binding affinities with good binding energies were obtained after coupling the ligands kaempferol and rutin to superoxide dismutase a2 (SOD) with the energies being − 8.1 kcal/mol and − 8.7 kcal/mol, respectively. Illustrations of the interactions observed after modeling kaempferol in the binding site of SOD, as seen in Fig. 6(A) shows that the key residues involved in this interaction are VAL5, CYS6, VAL7, LEU8, LYS9, GLY10, ASP11, ASN53, GLY56, CYS57, CYS146, GLY147, VAL148 and ILE149. In Fig. 5(B) and Fig. 5(C), the key residues interacting with rutin are CYS6, VAL7, LEU8, LYS9, GLY10, ASP11, GLY12, PRO13, VAL14, GLN15, ASN53, THR54, ALA55, GLY56, CYS57, ALA145, CYS146, GLY147 and VAL148. Fig. 6(B) also shows the key residues interacting with F chain residues in SOD indicated as CYS6, VAL7, LEU8, LYS9, GLY10, ASP11, GLY12, and GLN15. These interactions reveal a promising prospective therapy to be gained from utilizing rutin, kaempferol, and drugs containing any or both of these bioactive agents.

A docking study proves that rutin possesses the most negative interaction energy with superoxide dismutase (SOD) among the three chemicals. Rutin's binding energy is 8.7 kcal/mol, whereas kaempferol's binding energy is only –8.1 kcal/mol per mole. There is more interaction between rutin and the active site of SOD than between kaempferol and its active site. Exchangeable Hydrogens on SOD are more involved with rutin. More residues are interacting with rutin, and act in additional interaction with residues on the F chain. *In-silico* studies provide evidence that rutin is a superior chemical compared to both kaempferol and ascorbic acid in terms of its ability to modify SOD's activity (overall negative binding energy). Nevertheless, some of these

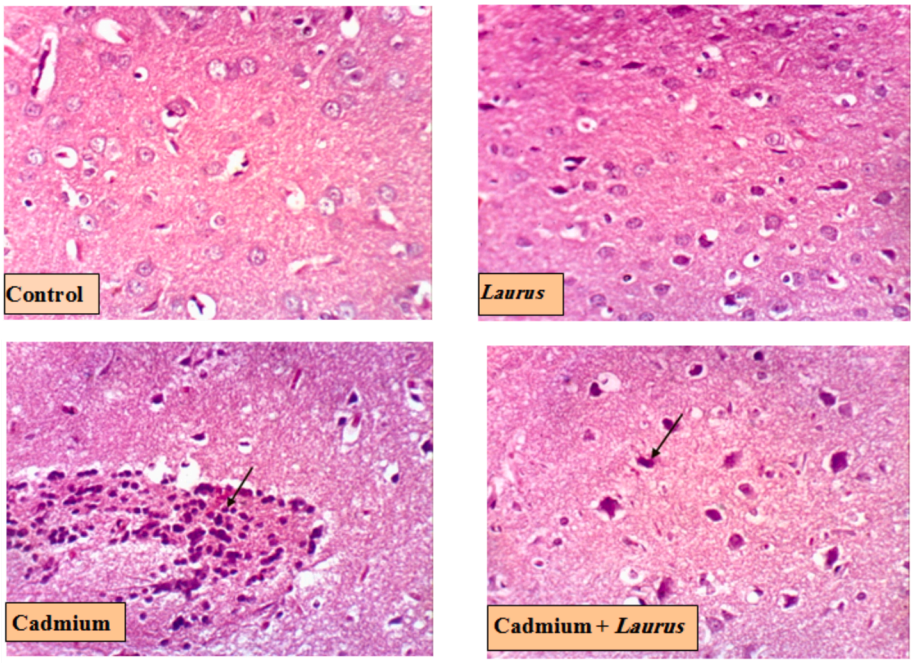

Fig. 4. Brain photomicrograph (cerebral cortex) for Control and treated groups (H & EX 400, Scale bar 50 μm).

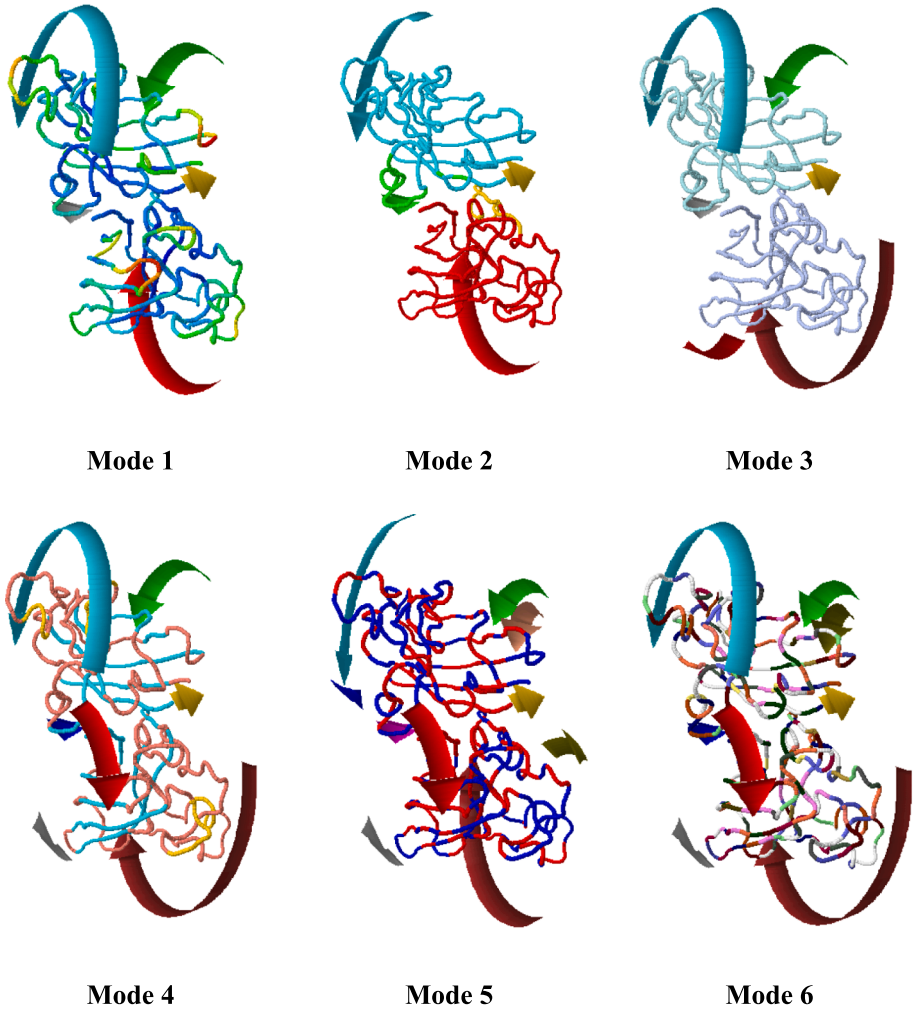

Fig. 5. SOD model different modes for rotation about verification of high degree of structural stability.

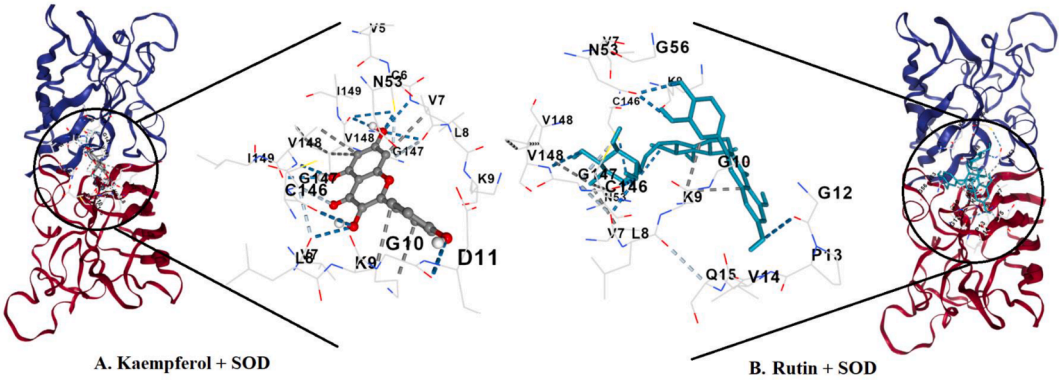

Fig. 6.

findings have yet to be investigated in the laboratory, or taken up to the in vivo level for convincing and persuasion.

3.10.3. PyLip interactions

PyLip Interactions within a protein structure, including metal complexes, hydrogen bonds, and water bridges. several observations were made regarding the interactions of kaempferol, rutin, or their interactions with Superoxide Dismutase A2 (SOD) within the protein structure, particularly focusing on metal complexes, hydrogen bonds, and water bridges as mentioned in the Supplementary File **(S1)**. The results detail provided encompasses analyses of metal complexes, hydrogen bonds, and water bridges within a protein structure as shown in Fig. 7. In the metal complexes section, two distinct complexes are examined: one involving copper (Cu) in a trigonal planar coordination environment, and the other involving zinc (Zn) in a trigonal bipyramidal coordination geometry. For the Cu complex, residues HIS 46A, HIS 48A, and HIS 120A are coordinated with distances of approximately 1.99 to 2.02 Å from the metal ion. Similarly, for the Zn complex, residues HIS

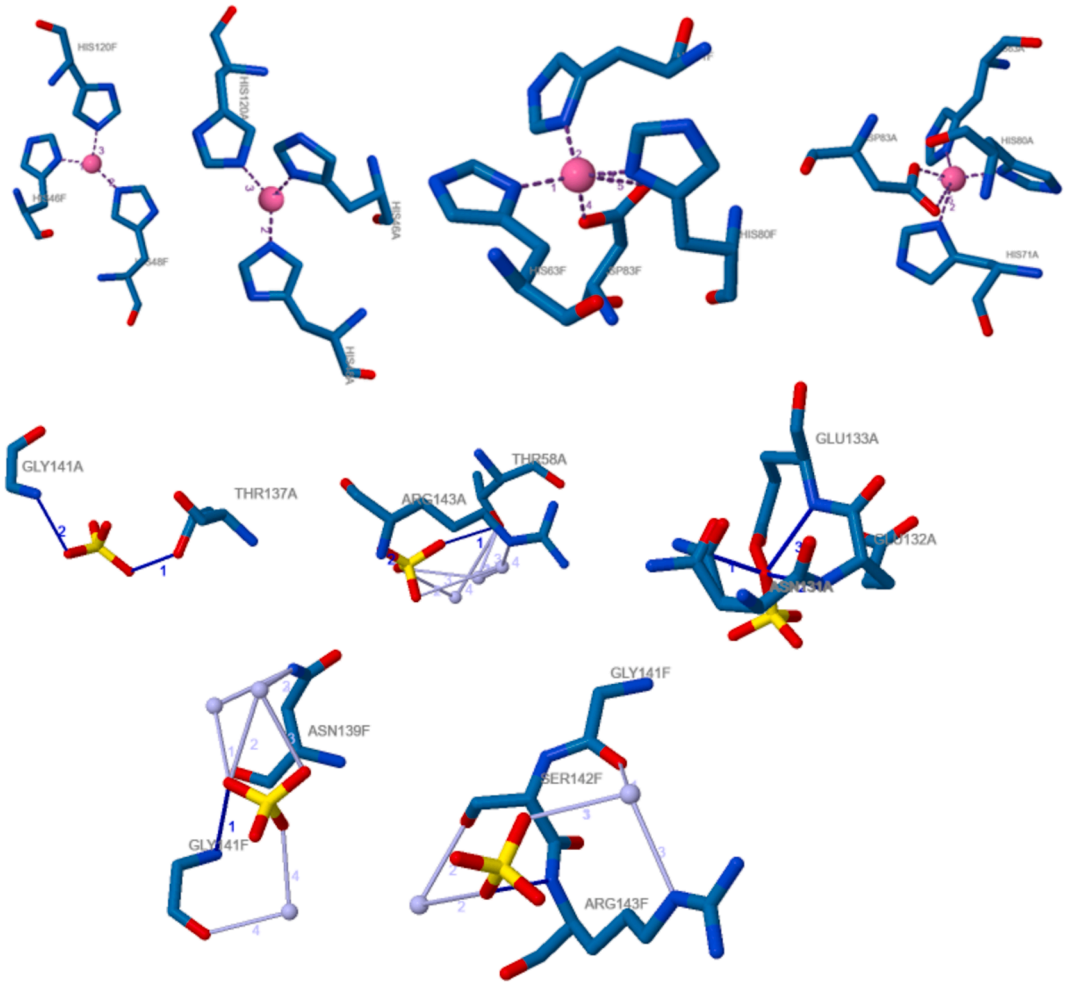

Fig. 7. Interaction of SOD with Kaempferol and Rutin.

63A, HIS 71A, HIS 80A, ASP 83A (twice), and ASP 83A (again, twice) coordinate with distances ranging from approximately 1.92 to 2.85 Å.

Hydrogen bonds, and interactions are noted between various residues and surrounding atoms. For example, THR 137A forms a hydrogen bond with a distance of approximately 2.50 Å to the donor atom and 2.87 Å to the acceptor atom, with a donor angle of around 102.56 degrees. Similar interactions are observed for GLY 141A, THR 58A, and ARG 143A. Lastly, water bridges are identified, indicating interactions between protein residues and water molecules. These bridges involve residues like THR 58A, ARG 143A, ASN 139F, GLY 141F, and SER 142F, with distances ranging from approximately 2.71 to 4.09 Å between the donor and water, and donor angles varying from around 101.61 to 158.84 degrees. These findings collectively provide insight into the structural features and interactions within the protein system under investigation

3.10.4. Comparative analysis of Solubility, Lipophilicity, and drug Likeness of Kaempferol and rutin

Solubility curves, lipophilicity parameters and chemical similarity analyzes of kaempferol and rutin show significant differences in their physicochemical and pharmacokinetic properties. The solubility curve according to Table 10 (A) shows that the Log S (ESOL) value of kaempferol is −3.31, indicating a solubility of 1.40e-01 mg/ml (4.90e-04 mol/l), which is classified as as: easily soluble. In contrast, rutin has a similar Log S value (ESOL) of −3.30 and a solubility of 3.08e-01 mg/ml (5.05e-04 mol/l), also classified as soluble. However, other solubility tests such as Log S (Ali) and Log S (SILICOS-IT) show that routine is slightly more soluble than Log S (SILICOS-IT). High resolution varies depending on the method used.:1.70, XLOGP3: 1.90, WLOGP: 2.28, MLOGP: −0.03, SILICOS-IT: 2.03), resulting in a consistent log Po/w of 1.58. This shows that the lipophilic environment is suitable for drug-like products. On the other hand, the negative log Po/w for the routine is −1.29, and all values vary significantly (iLOGP: 1.58, XLOGP3: −0.33, WLOGP: −1.69, MLOGP: −3.89, SILICOS- IT: − 2.11) will affect its permeability and absorption, reflecting its low lipophilicity.

Muegge law, no violation, bioavailability score 0.55. It also showed no warnings in the PAINS or Brenk test and was considered a leader with a combined range of 3.14. In contrast, rutin is incompatible with many similar chemicals, including Lipinski (three violations: molecular weight > 500, number of oxygen or nitrogen atoms > 10, number of hydrogen allocations > 5), Ghose (four violations: molecular weight > 480).), WLOGP < -0.4, molar refractive index > 130, atomic number > 70), Veber (one violation: topological polar surface > 140), Egan (one violation: TPSA > 131.6), and Muegge (four violations: Molecular weight) > 600, TPSA > 150, hydrogen bond acceptor > 10, hydrogen bond donor > 5). Rutin has a lower bioavailability score of 0.17; this stimulates all PAINS and Brenk tests due to its molecular weight of > 350, unlike lead, and a higher rating of 6.52 from electronic products, indicating that it is more difficult to synthesize. Although Rutin has a high solubility in some substances, it faces significant problems due to its poor lipophilicity, interference with many similar drugs, and lack of bioavailability, which may limit its ability as a drug candidate.

Table 10
Solubility Profile, Lipophilicity Parameters Analysis, and Drug Likeness Assessment of Kaempferol.

Table 2 **(A)**	**Solubility profile**	
Compounds	**Kaempferol**	**Rutin**
Log S (ESOL)	−3.31	−3.30
Solubility	1.40e-01 mg/ml; 4.90e-04 mol/l	3.08e-01 mg/ml; 5.05e-04 mol/l
Class	Soluble	Soluble
Log S (Ali)	−3.86	−4.87
Solubility	3.98e-02 mg/ml; 1.39e-04 mol/l	8.30e-03 mg/ml; 1.36e-05 mol/l
Class	Soluble	Moderately soluble
Log S (SILICOS-IT)	−3.82	−0.29
Solubility	4.29e-02 mg/ml; 1.50e-04 mol/l	3.15e + 02 mg/ml; 5.15e-01 mol/l
Class	Soluble	Soluble
Log S (ESOL)	−3.31	−3.30

Table 2(B)	**Lipophilicity Parameters Analysis**	
Compounds	**Kaempferol**	**Rutin**
Log Po/w (iLOGP)	1.70	1.58
Log Po/w (XLOGP3)	1.90	−0.33
Log Po/w (WLOGP)	2.28	−1.69
Log Po/w (MLOGP)	−0.03	−3.89
Log Po/w (SILICOS-IT)	2.03	−2.11
Consensus Log Po/w	1.58	−1.29
Log Po/w (iLOGP)	1.70	1.58

Table 2(C)	**Drug Likeness Assessment**	
Compounds	**Kaempferol**	**Rutin**
Lipinski	Yes; 0 violation	No; 3 violations: MW > 500, NorO > 10, NHorOH > 5
Ghose	Yes	No; 4 violations: MW > 480, WLOGP < -0.4, MR > 130, #atoms > 70
Veber	Yes	No; 1 violation: TPSA > 140
Egan	Yes	No; 1 violation: TPSA > 131.6
Muegge	Yes	No; 4 violations: MW > 600, TPSA > 150, H-acc > 10, H-don > 5
Bioavailability Score	0.55	0.17
PAINS	0 alert	1 alert: catechol_A
Brenk	0 alert	1 alert: catechol
Leadlikeness	Yes	No; 1 violation: MW > 350
Synthetic accessibility	3.14	6.52

3.10.5. Simulation analysis

The selected model allows a comprehensive examination of the molecular structure. The deformability values of the residues tend to increase with higher atomic numbers, as shown by the positive correlation observed in the plot of deformability and atomic index (Fig. 8A). The protein structure exhibits a remarkable level of flexibility, as evidenced by the range of deformability values, which range between 0.2 and 0.5. The self-analysis findings reveal that the protein structure exhibits a significant degree of flexibility, as demonstrated by the relatively high deformability scores. A closer analysis of the protein sequence reveals that areas exhibiting substantial sequence variability align with regions characterized by high deformability. This suggests that the protein could be undergoing conformational alterations to adapt to different binding partners. Residues with higher atomic numbers often exhibit higher B-factor values, as seen by the positive correlation observed between these two parameters in the plot of B-factor and atomic index (Fig. 8B).

The B factor values, ranging from 0 to 1, represent the level of thermal mobility or flexibility of the protein structure. The range of the MNA B factor, illustrated above, spans from 0.6 to 1, indicating a notable level of flexibility in this specific region. The PDB B factor ranges from 0.2 to 0.6, indicating a notable degree of flexibility in this region. According to a self-analysis, The protein structure reveals that areas with high crystallographic temperature factors correspond to regions with high B factors. This suggests that the protein may be undergoing thermal motion to facilitate binding or catalysis. Fig. 8 **(C)** shows the eigenvalues of −2.492433e-04, which represent the energy required to modify the level of stiffness and structure.

A lower eigenvalue means a lower degree of complex deformation. Deformation requires a specific amount of energy expenditure because the stiffness constant of the structure is 0.024. Fig. 8(D) shows the variance associated with each normal mode, ranging from 0.01 to 0.1. Individual (red) and cumulative (green) fluctuations combine to form a total variance of 0.5, indicating the level of adaptability and diversity of the structure. Fig. 8 **(E)** presents a covariance map with a correlation coefficient of 0.7. The map represents the correlation between pairs of residuals, with values ranging between −0.5 and 0.5. The data displayed exhibits a positive correlation (red), no correlation (white), or a negative correlation (blue). Fig. 8 **(F)** shows the elastic network paradigm, which defines the relationships between atoms using springs. The model provides a deep understanding of structural dynamics, stiffness, flexibility, and their relationships, with an average spring constant of 0.5. The stiffness of the points determines their tone. Points with higher grayscale values have stiffness values ranging from 0.1 to 1, while points with lighter grayscale values have stiffness values ranging from 0.01 to 0.1.

4. Discussion

The results of this study highlight the *Laurus* extract's strong capability to neutralize ABTS radicals, pointing to its potential in treating diseases related to free radicals. This aligns with the findings of Guenane et al. (2016), who also reported significant antioxidant activity of *Laurus* assessed by ABTS. Also the FRAP assay, assessing antioxidant reduction capacity, involves the interaction with ferric tripyridyltriazine (Fe3 −TPTZ) forming ferrous tripyridyltriazine (Fe2 −TPTZ) (Benzie and Strain 1996). The reduction properties are typically associated with hydrogen atom donors, disrupting free radical chains (Duh et al., 1999). These findings suggest that *Laurus* leaf extract's antioxidant properties could be effective in preventing diseases caused by free radicals, like those induced by cadmium toxicity in tissues such as the brain.

In this study The GC–MS analysis of the *Laurus* ethanol extract revealed various compounds, among these compounds is Hexadecanoic acid, methyl ester (methyl palmitate), an organic compound known for its antimicrobial, anticancer, anti-inflammatory, and insecticidal activities (Mohamed et al., 2021). Additionally, (Z)-13-Docosenamide, a long-chain fatty acid amide found in plants, insects, and mammals, has been researched for its biological activities and potential applications (Banc et al., 2023). This compound is noted for its anti-inflammatory properties, inhibiting pro-inflammatory molecules production, and has been suggested to have neuroprotective effects, potentially protecting neurons from damage due to oxidative stress and inflammation (Yang et al., 2021). Several studies have proposed potential neuroprotective effects of (Z)-13-Docosenamide. It is believed to shield neurons from damage induced by oxidative stress, inflammation, and other harmful factors, thereby potentially safeguarding neuronal health (Lee et al., 2020). Other compounds in the *Laurus* extract include Santamarine and Reynosin, sesquiterpene lactones with biological activities like anti-allergenic, anti-inflammatory, antispasmodic, and cytotoxic properties (Tucker and Debaggio, 2000; Harborne and H. Baxter et al., 1983; Duke,1992).

Several studies have highlighted the substantial influence of various flavonoids and other phenolic compounds on immune system function and inflammatory processes (Middleton and Kandaswami, 1992; Locatelli et al., 2018). The flavonoids quercetin, apigenin, and hesperidin have been identified as having possible anti-inflammatory properties (Pham-Huy et al., 2008). Quercetin, a member of the flavonol class, has

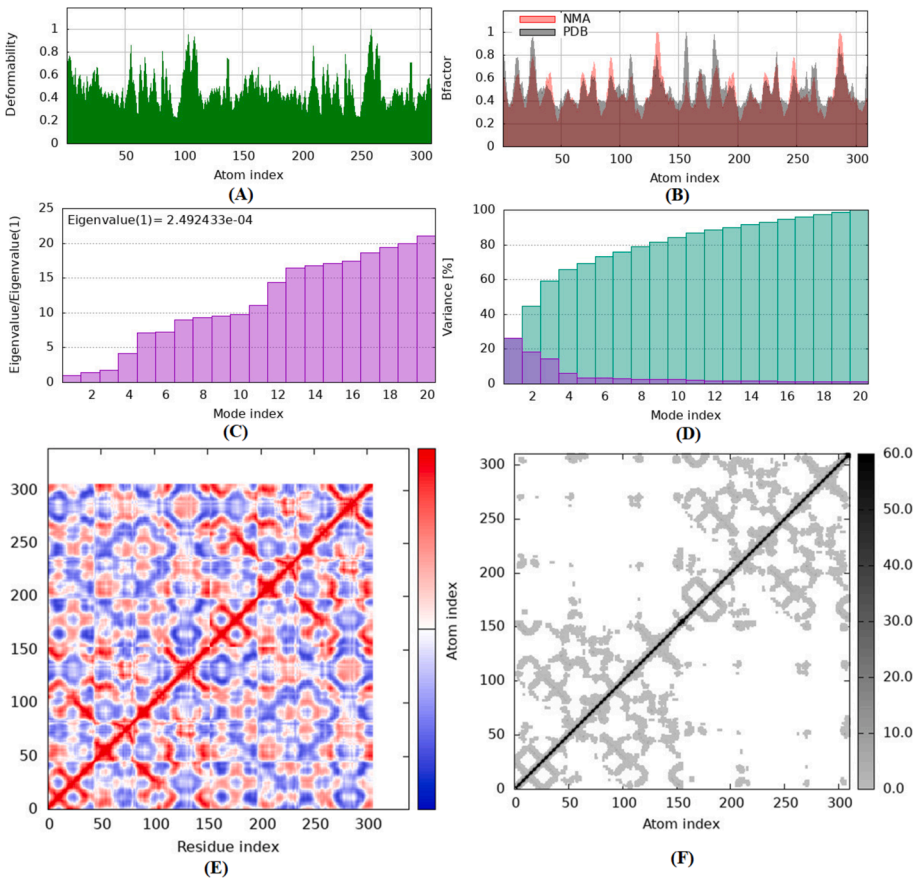

Fig. 8. A represents the model detail of Eigenvalues, B Variance, C Covariance Map and D shows Elastic Network.

been documented as a noteworthy substance with potential anticancer properties, particularly in relation to prostate and breast cancers (Pham-Huy et al., 2008; Brusselmans et al., 2005).

These findings highlight the crucial role that *Laurus* leaf extract, with its rich content of phenolic and flavonoid compounds, may play in health and disease management. The anti-inflammatory and potential anticancer properties of these compounds could be particularly beneficial in combating diseases associated with oxidative stress and inflammation, such as those induced by cadmium exposure.

In biological experiment results reported that Cd exposure led to a notable reduction in body weight gain and brain weight ($p < 0.05$) compared to the control group. This finding aligns with previous research on body weight and organ weights (Nnaa et al., 2017). Rahman et al. (1998) reported a direct association between long-term Cd exposure and an increased risk of type 2 diabetes, leading to weight loss in rats. Also, heavy metal exposure deteriorates the glucocorticoid system, correlated with weight gain/loss (Kaltreider et al. 2001). Most recent phytochemical studies reported phenolics, flavonoids, alkaloids, and numerous other biological activities in *Laurus* (Gazwi et al., 2020). These components support *Laurus* as natural antioxidant therapy of diseases caused by oxidative stress. The nutritional and calorific properties of *Laurus* may result in this improvement in weight (Shaba et al. 2015).

Donmez et al. (2019) and El-Boshy et al. (2015), who reported similar decreases in hematological parameters due to Cd toxicity. Cd exposure can lead to anemia by accumulating toxic metals in the kidney, spleen, and liver, causing peripheral RBC deformities and hemolysis (Kunimoto et al., 1985). Cd also adversely affects intestinal iron absorption, contributing to anemia.

This immune response alteration could result from diminished antioxidant activity and increased free radicals due to Cd exposure, as well as suppression of non-specific and systemic inflammation (Fahim et al. 2012).

On the other hand, *Laurus* treatment ameliorated these hematological alterations, showing protective effects against RBC degradation caused by Cd (Nazima et al. 2016). *Laurus* seems to exert a protective influence on the hematopoietic system, as evidenced by improvements in some hematological parameters and lymphocyte concentrations compared to the Cd group.

These results demonstrate the adverse effects of Cd on body weight, brain weight, and hematological parameters, while also highlighting the potential protective role of *Laurus* extract in mitigating these effects. This suggests the efficacy of *Laurus* as a therapeutic agent in conditions involving oxidative stress and toxicity. The results in this study are consistent with findings by Abu Al-Dhahab et al. (2019) and Prabu et al. (2012), who observed similar increases in ALT, AST, bilirubin, and ALP in Cd-treated mice. Altered renal enzyme levels reflect Cd-induced renal damage as noted by Bekheet et al. (2011). In another hand In contrast, *Laurus* extract was administered alongside cadmium, showed noticeable reductions or mitigations in these biomarker levels. This suggests a protective effect against oxidative stress and potential hepatorenal toxicity induced by cadmium exposure. These results highlight the potential therapeutic role of *Laurus* extract in ameliorating cadmium-induced oxidative stress in biological systems.

Antioxidants, known for their scavenging activity and ability to modulate antioxidant enzyme systems, are proposed to mitigate Cd-induced oxidative damage. Cd-induced reactive oxygen species (ROS) overproduction depletes both enzymatic (SOD and CAT) and non-enzymatic (GSH) antioxidants, disrupting antioxidant defenses (Li et al., 2017; Al Olayan et al., 2020; Al-Quraishy, 2020). Antioxidants protect against oxidative damage, but Cd exposure disrupts their activities, leading to immune imbalance (Seif et al., 2019 and Ishtiaq et al.,

2022).

Notably, *Laurus* ameliorated oxidative damage caused by Cd in brain tissue, as evidenced by reduced MDA levels and increased antioxidant proteins. These findings align with Gazwi et al. (2020), who reported the efficacy of *Laurus* as an antioxidant in rats exposed to heavy metals. Phytochemical analysis via GC–MS identified 13-Docosenamide (Z)-, also known as erucamide, as a major component in the extract. Erucamide is a long-chain unsaturated fatty acid amide known for its antinociceptive and anti-inflammatory properties [Shareef et al., 2016]. Additionally, hexadecanoic acid, methyl ester, another significant component of the extract, has been shown to possess neuroprotective qualities in rats by modulating cerebral blood flow [Lee et al., 2019]. Thus, the observed biological effects can be attributed to these key phytochemicals, which contribute to the antioxidant and neuroprotective properties of *Laurus* extract.

The reduction in AChE activity observed in our study is indicative of brain dysfunction, This finding aligns with the results of Al Olayan et al. (2020). Under oxidative stress, AChE activity diminishes, leading to the accumulation of ACh in the central nervous system (CNS). This buildup can result in increased neuronal excitability, manifesting as cholinergic hyperactivity, and potentially leading to epilepsy-like behavior and seizures (Tsakiris et al., 2000).Previous studies, such as those by Al Omairi et al. (2018), have demonstrated that Cd-induced changes in neurochemical transmission can lead to impaired brain function. as AChE plays a critical role in breaking down acetylcholine (ACh) in synapses into acetic acid and choline. This suggests that *Laurus* extract mitigates the toxic effects of Cd on AChE activity. Supporting this, Gazwi et al. (2020) found that polyphenols, known for their antioxidant properties, exhibit strong anti-AChE inhibitory activity (Dizdar et al., 2018). Histopathology examination of brain in this study are consistent with the observations of Al Olayan et al. (2020). Kaoud and Mekawy (2011) which appeared that there was necrosis of neurons in the Microphotograph of the brain in the cadmium group. The dangerous changes in the nerve cells are due to ROS's presence (Kuhad and Chopra, 2007). The protective effects of the *Laurus* extract are likely due to its antioxidant compounds that inhibit free radical formation and reduce their detrimental impact on neural tissue (Gazwi et al., 2020). Al Olayan et al. (2020) have suggested that antioxidants targeting neurotrophic factors could play a crucial role in safeguarding nervous tissue against Cd toxicity.

5. Conclusion

In conclusion, this study elucidates the detrimental effects of Cd exposure on neurological health and underscores the therapeutic efficacy of Laurus nobilis L. in mitigating Cd-induced neurotoxicity. The neuroprotective effects of Laurus extract are attributed to its antioxidant constituents, which scavenge free radicals, inhibit oxidative stress, and preserve neuronal integrity. The findings provide valuable insights into the use of Laurus as a potential therapeutic agent against heavy metal toxicity-induced neurodegenerative disorders. *In-slico* analysis shows that High resolution 2.05x structural analysis and identification of superoxide dismutase (SOD) were shown to be supported by positive R values (active: 0.192, free: 0.236, apparent: 0.194) and a C value of the molecular structure final 0.30. Docking studies showed that kaempferol (−8.1 kcal/mol) and rutin (−8.7 kcal/mol) have a strong affinity for SOD and key residues such as VAL5, CYS6, and ASP11 are involved in the interaction. Comparative analysis shows that kaempferol has a solubility of 1.40e-01 mg/ml, high lipophilicity (Log Po/w 1.58), and has no violations in drug-like tests and its bioavailability is better than routine when the routine faces many violations. Low simulation analysis showed protein variation indicated by strain values (0.2–0.5) B factor ranges (0–1) and eigenvalues (−2.492433e-04), indicating the adaptability of the protein and the potential for future research. This comprehensive review confirms the reliability and therapeutic potential of SOD, especially kaempferol, as a promising drug candidate. Further research is warranted to elucidate the underlying mechanisms and optimize dosage regimens for clinical applications.

Consent to participate

Not applicable.

Consent for publication

Not applicable.

Authors contribution

Hanaa M. Hassan, Hanaa S.S Gazwi , and Eman E. Yassien conceived the project. Hanaa M. Hassan, Hanaa S.S Gazwi, Asmaa Hussein Zaki, and Eman E. Yassien designed and per-formed the experiments. Hanaa M. Hassan, Hanaa S.S Gazwi , Asmaa Hussein Zaki, and Eman E. Yassien analyzed the data. Hanaa S.S Gazwi , Hanaa M. Hassan, Asmaa Hussein Zaki, Marija Milošević, Salim S. Al-Rejaie, Mohamed Mohany and Eman E. Yassien wrote the manuscript. Hanaa S.S Gazwi, Hanaa M. Hassan, Asmaa Hussein Zaki, Marija Milošević, Salim S. Al-Rejaie, Mohamed Mohany , and Eman E. Yassien provided critical discussion, editing, and final approval of the manuscript. All authors contributed to the preparation of the manuscript. All authors have read and agreed to the published version of the manuscript.

Funding

This work was funded by the Researchers Supporting Project (RSPD2024R758), King Saud University, Riyadh, Saudi Arabia.

CRediT authorship contribution statement

Hanaa M. Hassan: Writing – review & editing, Writing – original draft, Supervision, Resources, Project administration, Methodology, Investigation, Funding acquisition, Formal analysis, Data curation, Conceptualization. **Hanaa S.S. Gazwi:** Writing – review & editing, Writing – original draft, Visualization, Validation, Supervision, Software, Resources, Project administration, Methodology, Investigation, Formal analysis, Data curation, Conceptualization. **Inas Hussein Refaat:** Writing – review & editing, Writing – original draft, Project administration, Methodology. **Asmaa Hussein Zaki:** . **Marija Milošević:** Writing – review & editing, Writing – original draft, Visualization, Project administration, Methodology, Investigation, Data curation. **Salim S. Al-Rejaie:** Writing – review & editing, Writing – original draft, Visualization, Validation, Supervision, Resources, Project administration, Investigation, Funding acquisition, Formal analysis, Data curation. **Mohamed Mohany:** Writing – review & editing, Writing – original draft, Software, Methodology, Investigation, Data curation. **Eman E. Yassien:** Writing – review & editing, Writing – original draft, Formal analysis, Data curation, Conceptualization.

Declaration of competing interest

The authors declare that they have no known competing financial interests or personal relationships that could have appeared to influence the work reported in this paper.

Acknowledgment

The authors extend their appreciation to the Researchers Supporting Project (RSPD2024R758), King Saud University, Riyadh, Saudi Arabia.

Appendix A. Supplementary data

Supplementary data to this article can be found online at https://doi.

org/10.1016/j.jksus.2024.103488.

References

Abu-El-Zahaba, H.S.H., Hamza, R.Z., Montaserd, M.M., El-Mahdia, M.M., Al-Harthic, W. A., 2019. Antioxidant, antiapoptotic, antigenotoxic, and hepatic ameliorative effects of L-carnitine and selenium on cadmium-induced hepatotoxicity and alterations in liver cell structure in male mice. Ecotoxicol. Environ. Saf. 173, 419–428.

Adams, R.P., 2007. Identification of Essential Oil Components by Gas Chromatography/ Mass Spectrometry, 4th Edition. Allured Publishing Corporation, Carol Stream.

Aebi, H., 1984. Catalase in vitro. Methods Enzymol. 105, 121–126.

Al Olayan, E.M., Aloufi, A.S., AlAmri, O.D., El-Habit, O.H., Abdel Moneim, A.E., 2020. Protocatechuic acid mitigates cadmium-induced neurotoxicity in rats: Role of oxidative stress, inflammation and apoptosis. Sci. Total Environ. 723, 137969.

Al Omairi, N.E., Radwan, O.K., Alzahrani, Y.A., Kassab, R.B., 2018. efficiency of Mangifera indica leaves extract on cadmium-induced cortical damage in rats. Metab. Brain Dis. 33, 1121–1130.

Almeer, R.S., AlBasher, G.I., Alarif, S., Alkahtani, S., Ali. Abdel Moneim, A. E., 2019. Royal jelly attenuates cadmium induced nephrotoxicity in male mice. Sci. Rep. 9, 5825.

Al-Quraishy, S., Dkhil, M.A., Abdel-Gaber, R., Zrieq, R., Hafez, T.A., Mubaraki, M.A., Abdel, M.A., E., 2020. Myristica Fragrans Seed Extract Reverses Scopolamine-Induced Cortical Injury via Stimulation of HO-1 Expression in Male Rats. Environ Sci Pollut Res 07686–07688.

Arnao, M.B., Cano, A., Acosta, M., 2001. The hydrophilic and lipophilic contribution of total antioxidant activity. Food Chem. 73, 239–244.

ATSDR Support document to the (2022) substance priority list (candidates for toxicological profiles) agency for toxic substances and disease registry division of toxicology and human health sciences December 2022 1–12.

Banc, R., Rusu, M.E., Filip, L., Popa, D.-S., 2023. Phytochemical Profiling and Biological Activities of Quercus sp. Galls (Oak Galls): A Systematic Review of Studies Published in the Last 5 Years. Plants 12, 3873.

Banchroft, J. D., Stevens A. m Turner D. R. (1996). Theory and practice of histological techniques.Fourth Ed. Churchil Livingstone, New York, London, San Francisco, Tokyo.

Bekheet, S.H., Awadalla, E.A., Salman, M.M., Hassan, M.K., 2011. Bradykinin potentiating factor isolated from Buthus occitanus venom has a protectiveeffect against cadmium induced rat liver and kidney damage. Tissue Cell 43, 337–343.

Belfield, A., Goldberg, D., 1971. Colorimetric determination of alkaline phosphatase activity. Enzyme 12, 561–566.

Benzie, I.F., Strain, J.J., 1996. The ferric reducing ability of plasma (FRAP) as a measure of "antioxidant power": The FRAP assay. Anal. Biochem. 239, 70–76.

Chaudhry, N.M., Tariq, P., 2006. Bactericidal activity of black pepper, bay leaf, aniseed and coriander against oral isolates. Pak. J. Pharm. Sci. 19, 214–218.

Dacie, J.V., Lewis, S.M., 1991. Practical Haematology, 7th. ELBS with Churchill Livingstone, Edinburgh, pp. 37–85.

Deng, P., Zhang, H., Wang, L., Jie, S., Zhao, Q., Chen, F., Yue, Y., Wang, H., Tian, L., Xie, J., Chen, M., Luo, Y., Yu, Z., Pi, H., Zhou, Z., 2023. Long-term cadmium exposure impairs cognitive function by activating lnc-Gm10532/m6A/FIS1 axis-mediated mitochondrial fission and dysfunction. Sci. Total Environ. 858, 159950.

Dizdar, M., Vidic, D., Požgan, F., Štefane, B. and Maksimović, M (2018). Acetylcholinesterase Inhibition and Antioxidant Activity of N-trans-Caffeoyldopamine and N-trans-Feruloyldopamine. Sci Pharm. Apr 4;86(2):11.

Donmez, H.H., Donmez, N., Kısadere, I., Undag, I., 2019. Protective effect of quercetin on some hematological parameters in rats exposed to cadmium. Biotech. Histochem. 94, 381–386.

Draper, H., Hadley, M., 1989. Malondialdehyde determination as index of lipid peroxidation. Methods Enzymol. 186, 421–431.

El-Boshy, M.E., Risha, E.F., Abdelhamid, F.M., Mubarak, M.S., Hadda, T.B., 2015. Protective effects of selenium against cadmium induced hematological disturbances, immunosuppressive, oxidative stress and hepatorenal damage in rats. J Trace Elem Med. 29, 104–110.

Ellman, G.L., Courtney, K.D., Andres Jr., V., Feather-Stone, R.M., 1961. A new and rapid colorimetric determination of acetylcholinesterase activity. Biochem. Pharmacol. 7, 88–95.

Fahim, M.A., Nemmar, A., Dhanasekaran, S., Singh, S., Shafiullah, M., Yasin, J., Zia, S., Hasan, M.Y., 2012. Acute cadmium exposure causes systemic and thromboembolic events in mice. Physiol Res. 61, 73–80.

Fawcett, J.K., Scott, J.E., 1960. Determination of urea by method using Berthelot reaction. J. Clin. Pathol. 13, 156.

Gazwi, H.S.S., Yassien, E.E., Hassan, H.M., 2020. Mitigation of lead neurotoxicity by the ethanolic extract of *Laurus* leaf in rats. Ecotoxicol. Environ. Saf. 1, 192:110297.

Genchi, G., Sinicropi, M.S., Lauria, G., Carocci, A., Catalano, A., 2020. The effects of cadmium toxicity. Int. J. Environ. Res. Publ. Health 17.

Guenane, H., Gherib, A., Carbonell-Barrachina, Á., Cano-Lamadrid, M., Krika, F., Berrabah, M., Maatallah, M., Bakchiche, B., 2016. Minerals analysis, antioxidant and chemical composition of extracts of *Laurus nobilis* from southern Algeria. J. Mater. Environ. Sci. 7, 4253–4261.

Hassan, H.M., AbdElsabor, R.G., Sadeek, R.A., 2019. (2019) Potential ameliorative effects of garlic and onion by-products against the toxicity of ibuprofen in rats. Journal of Research in Specific Sciences and Arts, Alexandria- University. 11 (3), 74–98.

Kaltreider, R.C., Davis, A.M., Lariviere, J.P., Hamilton, J.W., 2001. Arsenic alters the function of the glucocorticoid receptor as a transcription factor. Environ. Health Perspect. 109, 245–251.

Kaoud, H. A. , Mekawy, M. M. (2011). Effect of Cadmium Pollution on Neuromorphology and Function of brain in Mice Offspring, Nature and Science, 2011; 9(4).

Kuhad, A., Chopra, K., 2007. Curcumin attenuates diabetic encephalopathy in rat: behavioral and biochemical evidence. Eur. J. Pain 576, 34.

Kunimoto, M., Miura, T., Kubota, K., 1985. An apparent acceleration of age-related changes of rat red blood cells by cadmium. Toxicol Appl Pharmacol. 77, 451–457.

Lee, R.H.C., Silva, A.C., Possoit, H.E., et al., 2019. Palmitic acid methyl ester is a novel neuroprotective agent against cardiac arrest. Prostaglandins Leukot Essent Fat Acids 147, 6–14.

Li, X., Jiang, X., Sun, J., Zhu, C., Li, X., Tian, L., Liu, L., Bai, W. (2017). Cytoprotective effects of dietary flavonoids against cadmium-induced toxicity. Ann N Y Acad Sci. 2017 Jun;1398(1):5-19.

Ma, Y., Su, Q., Yue, C., Zou, H., Zhu, J., Zhao, H., Song, R., Liu, Z., 2022. The effect of oxidative stress-induced autophagy by cadmium exposure in kidney, liver, and bone damage, and neurotoxicity. Int. J. Mol, Sci, p. 23.

Malti, J.E.L., Amarouch, H., 2009. Antibacterial effect, histological impact and oxidative stress studies from *Laurus* nobilis extract. J. Food Qual 32, 190–208.

Mohamed, Sh., Mohamed, G., Sara, F., 2021. Antibacterial activities of hexadecanoic acid methyl ester and green synthesized silver nanoparticles against multidrug resistant bacteria. J. Basic Microbiol. 61.

Motulsky, H. J. (1999). Analyzing Data with GraphPad Prism, GraphPad Software Inc., San Diego CA, www.graphpad.com.

Murray, R.L., 1984. Creatinine Kaplan A Clinical Chemistry. The C.V. Mosby Co., St. Louis. Toronto. Princeton 418, 1261.

Nazima, B., Manoharan, V., Miltonprabu, S., 2016. Oxidative stress induced by cadmium in the plasma, erythrocytes and lymphocytes of rats: attenuation by grape seed proanthocyanidins. Hum Exp Toxicol. 35, 428–447.

Nishikimi, M., Roa, N.A., Yogi, K., 1972. The occurrence of superoxide anion in the reaction of reduced phenazine methosulfate and molecular oxygen. Biochem. Biophys. Res. Commun. 46, 849–854.

Nnaa, V.U., Ujaha, G.A., Mohamedb, M., Etima, K.B., Igbaa, B.O., Augustinea, E.R., Osima, E.E., 2017. Cadmium chloride–induced testicular toxicity in male wistar rats; prophylactic effect of quercetin, and assessment of testicular recovery following cadmium chloride withdrawal. Biomed. Pharmacother. 94, 109–123.

Pamphlett, R., Bishop, D.P., Kum Jew, S., Doble, P.A., 2018. Age-related accumulation of toxic metals in the human locus ceruleus. PLoS One 13, 0203627.

Rahman, M., Tondel, M., Ahmad, S.A., 1998. Diabetes mellitus associated with arsenic exposure in Bangladesh. Am. J. Epidemiol. 148 (2), 198–203.

Ravindran, C.A., Murugaiyah, V., Khiang, P.K., Xavior, R., 2013. Hepatopro-tective activity of leaf of methanol extract of *Laurus* nobilis L. againstparacetamol induced hepatotoxicity in rats. Asian J. Pharmaceut. Clin. Res. 6, 153–157.

Reitman, S., Frankel, S., 1957. A colourimetric method for the determination of serum oxaloacetic and glutamic pyruvic transaminases. Am. J. Clin. Path 28, 56–63.

Renugadevi, J., Prabu, S.M., 2010. Cadmium-induced hepatotoxicity in rats and the protective effect of naringenin Exp. Toxicol. Pathol. 62, 171–181.

Ruczaj, A., Brźoska, M.M.,, 2023. Environmental exposure of the general population to cadmium as a risk factor of the damage to the nervous system: a critical review of current data. J. Appl. Toxicol. 43, 66–88.

Sasaki, N., Carpenter, D.O., 2022. Associations between metal exposures and cognitive function in American older adults. Int. J. Environ. Res. Publ, Health, p. 19.

Schalm, O.W., jain N.C., Carroll E.J., 1975. Veterinary Haematology 3rded. Lea and Febiger, Philadelphia, pp. 66–180.

Shaba, E.Y., Ndamitso, M.M., Mathew, J.T., Etsunyakpa, M.B., Tsado, A.N., Muhammad, S.S., 2015. Nutritional and anti-nutritional composition of date palm (*Phoenix dactylifera L.)* fruits sold in major markets of Minna Niger state. Nigeria African J. Pure Appl. Chem. 9, 167–174.

Shareef, H., Haidar, J., Hussein, H., Hameed, I., 2016. Antibacterial effect of ginger (Zingiber officinale) Roscoe and bioactive chemical analysis using gas chromatography mass spectrum. Orient J Chem. 32),817–37.

Sunderman, F.W.J., 2001. Nasal toxicity, carcinogenicity, and olfactory uptake of metals. Ann. Clin. Lab. Sci. 31, 3–24.

Thevenod, F., Fels, J., Lee, W.K., Zarbock, R., (2019). Channels, transporters and receptors for cadmium and cadmium complexes in eukaryotic cells: myths and facts. Biometals 32, 469–489.

Tsakiris, S., Angelogianni, P., Schulpis, K.H., Stavridis, J.C. (2000) Protective effect of L-phenylalanine on rat brain acetylcholinesterase inhibition induced by free radicals. Clin Biochem. Mar; 33(2):103-106.

VanKampen, E.J., d Zijlstra, W. G., 1961. Standardization of hemoglobinometry. II. The Hemiglobincyanide Method. Clin Chim Acta 6, 538–544.

Vardapetyan, H., Tiratsuyan, S., Hovhannisyan, A., Rukhkyan, M., Hovhannisyan, D., 2013. Phytochemical composition and biological activity of *Laurus* nobilis L. leaves collected from two regions of South Caucasus. Journal of Experimental Biology and Agricultural Sciences 1, 45–51.

Walters, M.I., Gerarde, H.W., 1970. An ultramicromethod for the determination of conjugated and total bilirubin in serum orplasma. Microchem J 15, 231–243.

Wang, H., Matsushita, M.T., 2021. Heavy metals and adult neurogenesis. Curr. Opin. Toxicol. 26, 14–21.

Wu, L.C., Hsu, H.W., Chen, Y.C., Chiu, C.C., Lin, Y.I., Ho, J.A., 2006. Antioxidant and ant proliferative activities of red pitaya. Food Chem. 95, 319–327.

Yang, C., Chen, A., Chen, Y., 2021. College students' stress and health in the COVID-19 pandemic: the role of academic workload, separation from school, and fears of contagion. PLoS One 16, 0246676.